tvst

https://doi.org/10.1167/tvst.8.3.54

Article

High-Resolution In Vivo Fundus Angiography using a Nonadaptive Optics Imaging System

Mali Okada[1,2], Tjebo F. C. Heeren[2,3], Pádraig J. Mulholland[2–4], Peter M. Maloca[2,5–7], Marketa Cilkova[3], Vincent Rocco[2], Marcus Fruttiger[3], Catherine A. Egan[2,3], Roger S. Anderson[2–4], and Adnan Tufail[2,3]

[1] Royal Victorian Eye and Ear Hospital, Melbourne, Australia
[2] Moorfields Eye Hospital NHS Foundation Trust, London, UK
[3] Institute of Ophthalmology, University College London, London, UK
[4] Optometry and Vision Sciences Research Group, School of Biomedical Science, Ulster University, Coleraine, Northern Ireland
[5] OCTlab, Department of Ophthalmology, University Hospital Basel, Basel, Switzerland
[6] Institute of Molecular and Clinical Ophthalmology Basel (IOB), Basel, Switzerland
[7] Department of Ophthalmology, University of Basel, Basel, Switzerland

Correspondence: Adnan Tufail, Moorfields Eye Hospital NHS Trust, 162 City Road, London, UK. e-mail: adnan.tufail@nhs.net

Received: 28 December 2018
Accepted: 1 March 2019
Published: 27 June 2019

Keywords: fundus angiography; high-resolution; retinal imaging; fluorescein angiography

Citation: Okada M, Heeren TFC, Mulholland PJ, Maloca PM, Cilkova M, Rocco V, Fruttiger M, Egan CA, Anderson RS, Tufail A. High-resolution in vivo fundus angiography using a nonadaptive optics imaging system. Trans Vis Sci Tech. 2019;8(3):54, https://doi.org/10.1167/tvst.8.3.54

Purpose: We provide a proof of concept for the detailed characterization of retinal capillary features and surrounding photoreceptor mosaic using a customized nonadaptive optics angiography imaging system.

Methods: High-resolution fluorescein angiography (FFA) and/or indocyanine green angiography (ICGA) images were obtained using a modified Heidelberg retina angiograph (HRA2) device with a reduced scan angle enabling 3° field of view. Colocalized images of the photoreceptor mosaic also were captured in vivo using the same instrument. Visibility of vascular subbranches were compared between high-resolution images and conventional fundus angiography (FA) with a 30° field of view.

Results: High-resolution angiographic and infrared images (3° × 3° field of view, a 10-fold magnification) were obtained in 10 participants. These included seven patients with various retinal diseases, including myopic degeneration, diabetic retinopathy, macular telangiectasia, and central serous chorioretinopathy, as well as three healthy controls. Images of the retinal vasculature down to the capillary level were obtained on angiography with the ability to visualize a mean 1.2 levels more subbranches compared to conventional FA. In addition, imaging of the photoreceptor cone mosaic, to a sufficient resolution to calculate cone density, was possible. Movement of blood cells within the vasculature also was discernible on infrared videography.

Conclusions: This exploratory study demonstrates that fast high-resolution angiography and cone visualization is feasible using a commercially available imaging system.

Translational Relevance: This offers potential to better understand the relationship between the retinal neurovascular system in health and disease and the timing of therapeutic interventions in disease states.

Introduction

Fundus fluorescein angiography (FFA) was first described by Novotny and Alvis in 1961,[1] and has since become the gold standard imaging technique for assessing macular and retinovascular disorders. Along with indocyanine green angiography (ICGA) for examining the choroidal circulation, FFA has been instrumental in developing our understanding of the pathogenesis of many retinal and choroidal diseases. However, fundus angiography (FA) in its current form has several limitations. Although recent advances have been made with ultrawide field angiography,

the resolution of FA remains a limiting factor for studying microscopic features of the retinal vasculature and associated neuroretina.

In the search for accessible higher resolution retinal imaging, optical coherence tomography angiography (OCTA) is an emerging imaging modality that has been proposed as an alternative to FA for mapping retinal vessels. It is noninvasive and provides detailed delineation of the retinal capillary beds. However, it is subject to projection and motion artefacts, and the current technology is unable to demonstrate flow or leakage.[2] In addition, although OCTA provides some structural information about the neuroretina, this is not at the cellular level (e.g., photoreceptor mosaics).

An adaptive optics (AO)–based imaging system is another approach that has demonstrated great potential for imaging the retinal vasculature down to the capillary level.[3,4] This method has been used widely to investigate the neuroretinal structure, principally cone photoreceptor mosaics.[3–5] Two methods of adaptive optics scanning light ophthalmoscopy (AOSLO) system have been used to image retinal vessels, including a confocal system combined with oral fluorescein, as well as a nonconfocal AOSLO system, which is coupled with motion contrast to remove the need for contrast agents.[6–8]

Although these AO-based imaging systems provide unparalleled resolution of the retinal microstructure, they are complex, expensive, and require significant patient cooperation and image processing. As such, it currently is impractical to use in routine clinical practice or in large-scale clinical trials. A simpler, non-AO–based system that can resolve images in vivo down to the level of photoreceptors and small retinal capillaries has the potential to provide novel insights into retinal disease and may provide endpoints for future clinical studies. The ability to image larger numbers of patients with various levels of disease than is feasible using current AO systems also would help to generate new biomarkers in our understanding of retinovascular diseases. Although we demonstrated previously that the paramacular cone mosaic may be imaged in vivo using a modified scanning laser ophthalmoscope,[9,10] the capabilities of the device to provide high resolution angiography have not been examined. Therefore, we provide a proof-of-concept demonstration of high-resolution angiography alongside photoreceptor imaging using a modified commercially available nonadaptive optics imaging device.

Methods

Participants

Participants for this exploratory study were recruited from the medical retina clinics at Moorfields Eye Hospital. They were invited to join the study if they had retinal pathology requiring FFA and/or ICGA diagnostic workup as part of their clinical care. Additional healthy control participants also were recruited for comparative purposes. Participants were excluded if they had an allergy to intravenous dye, were less than 18 years old, or had significant media pathology that would preclude good quality imaging on conventional FA.

Ethics approval was obtained by the local institutional review board and the study was conducted according to the tenets of the Declaration of Helsinki. Written informed consent was obtained from all participants.

High-Resolution FA

High-resolution imaging was performed using a modified Heidelberg Retina Angiograph 2 (HRA2; Heidelberg Engineering GmbH, Heidelberg, Germany). This modification has been described previously for use in cone imaging by our team.[9] In summary, the standard scan angle of a conventional HRA2 was reduced by a factor of ×10, from 30° field of view down to 3°, with the narrow angle enabling a magnification of the image while retaining the same 768 × 768 density of pixels (Fig. 1). The field of imaging was 3° × 3°, which corresponds to an area on the retina of 0.825 × 0.825 mm, when calculated using standardized conversion rates at equivalent retinal loci.[11] The original commercial filters for FFA and ICG in the HRA2 were left in situ. The incident beam power, however, of the blue laser (488 nm) used for FFA and for blue reflectance imaging was reduced to 100 μW to meet the requirements for Class 1 emission limit according to the International Electrotechnical Commission 60825-1 guidelines. The high-resolution ICGA was acquired with the standard diode laser emitting 785 nm, with no change to laser output needed to meet safety guidelines. Cone imaging of the same location also was obtained using the infrared laser, but with the image acquisition set to reflectance mode. Near infrared autofluorescence (IRAF) also was performed in some patients to attempt to image the retinal pigment epithelium and choriocapillaris layer.

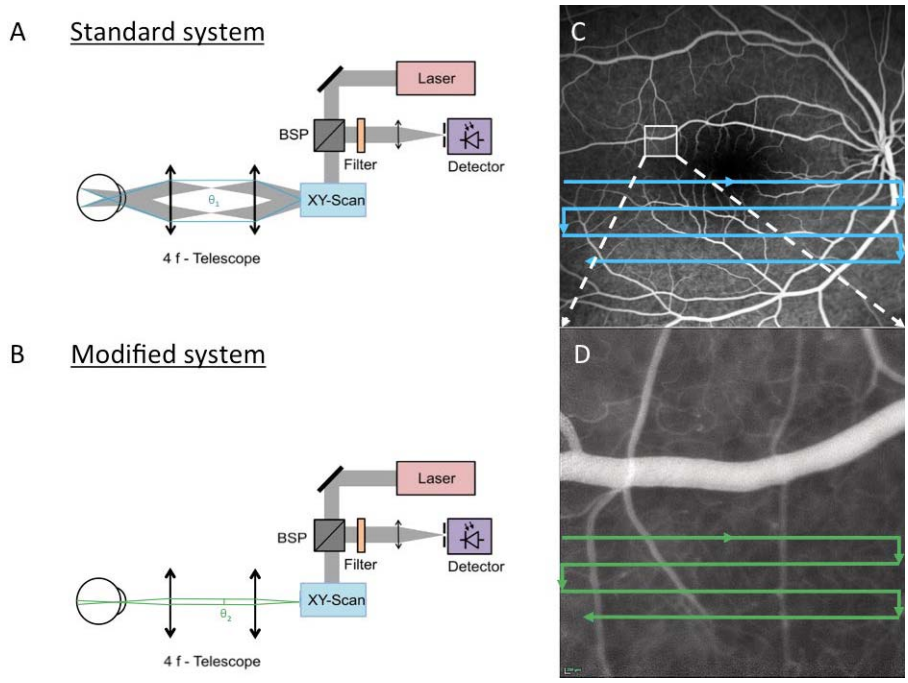

Figure 1. Schematic of (A) conventional Heidelberg HRA2 device with standard scanning angle (θ_1) and (B) modified high-resolution device with reduced scan angle (θ_2). (C) High resolution image with a scan angle of 3° superimposed onto conventional image of 30°.

Imaging Protocol

In vivo imaging was performed through dilated pupils with different areas of the fundus imaged by adjustment of the internal fixation lights. Standard doses of either 2 to 3 mL 20% sodium fluorescein dye or 25 mg/5 mL indocyanine green dye were injected for FFA and ICGA, respectively. Based on the clinical indication for the conventional FA, the majority of participants had early phase angiography images conducted on a conventional nonmodified HRA2 device with late phase images (>5 minutes) on the high-resolution device. This was done to have conventional and high resolution FA performed in the same sitting. In one participant, imaging was performed on three FA devices to enable comparisons across different imaging platforms: conventional HRA2, high-resolution HRA2, and Topcon TRC-NW8 retinal camera (Topcon Medical Systems, Inc., Oakland, NJ). In each participant, the device then was switched to infrared reflectance mode to capture the cone mosaic pattern at the same location as the FA imaging. Single, nonaveraged images as well as averaged real time (ART) images of 10 to 40 frames were acquired for conventional and high-resolution images. Videography also was obtained to record blood flow.

Image Analysis

Raw images were exported from Heidelberg Eye Explorer with the image borders cropped to remove other features (e.g., date information, patient-identifying data). The high-resolution images, comprising a 3° × 3° field (768 × 768 pixels), were exported into Adobe Photoshop CS 5.1 (Adobe Systems, Inc., CA) and scaled to size to enable manual overlay onto the corresponding conventional image for localization and comparison (Fig. 2).

A single grader masked to the origin of the images compared the conventional and high-resolution images separately for each patient. A qualitative assessment based on the clarity of large vessels as

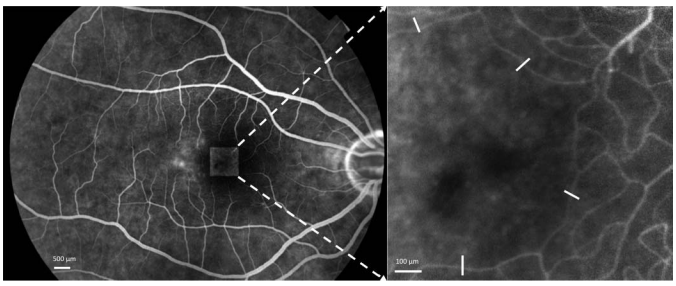

Figure 2. Localization and scaling of conventional (A) and high-resolution (B) images. Measurement of axial capillary diameter along various edged of the foveal avascular zone (C).

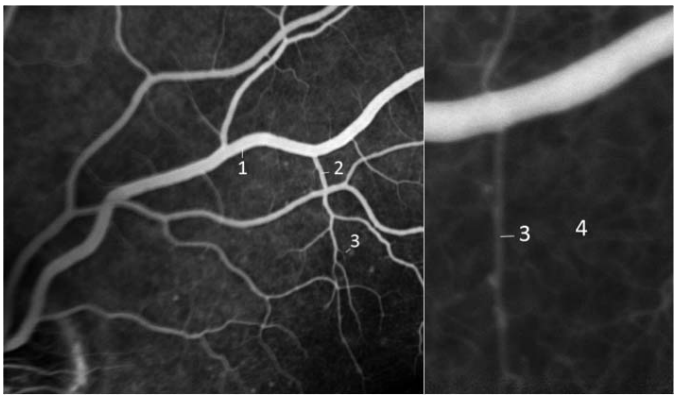

Figure 3. Grading scheme of retinal vasculature into subbranches of progressively smaller caliber.

well as a quantitative analysis by the visibility of subbranches off the main retinal vascular arcade at the same location with hierarchical numbering from branch 1 indicating main retinal arcade and 4 indicating capillary network (Fig. 3). Raw images were used for grading without adjustment for contrast. The difference between the two sets of images was calculated with a higher number indicating a step further in the hierarchy of vascular branching. The diameter of retinal capillaries along the foveal avascular zone (FAZ) rim edge also was examined for one participant. Four points along the FAZ rim were selected randomly, and the mean capillary diameter at these points was calculated (Fig. 2C).

Quantitative analysis of the cone photoreceptor array was performed using MATLAB software (R2014b; MathWorks, Inc., Natick, MA), according to the automated method described by Li and Roorda for use in AO images.[12] In brief, raw output images were cropped such that regions of the images containing no blood-vessels were isolated and a low-pass filter then applied in the frequency domain. The image then was converted back to the spatial domain and maximum local luminance was detected and plotted as cone centers, ensuring that identified cones were not closer than physiologically possible. Manual refinement of automated cone counts also was performed by a trained observer to account for cones detected erroneously. Voronoi analysis was subsequently performed, the results of this facilitating the assessment of cone packing arrangement (reported as the percentage of nonedge cells that demonstrate hexagonal packing), and inter-photoreceptor spacing (reported as a mean value in μm).

Results

A total of 10 participants (mean age, 47.5 years; range, 27–77; five male, 50%) were enrolled in the study. The demographic features and diagnosis for each participant are listed in Table 1. All patients tolerated the imaging well.

FFA and ICGA

In contrast to the standard images, the high-resolution images demonstrated greater visualization of smaller caliber vessels including its subbranches (mean 1.2 greater subbranches visible, median of 1 level, range 0–2; Table 2). In the participant with FFA performed on three different FA devices, the highest resolution, as determined by visibility of subbranches, was seen in the modified HRA2 device, followed by

Table 1. Clinical Characteristics of Participants

Participant	Age, Years	Sex	Right BCVA, Snellen	Left BCVA, Snellen	Diagnosis
1	68	F	6/6	6/7.5	Macular telangiectasia type 2
2	36	M	6/4	6/4	Central serous chorioretinopathy
3	58	M	6/9.5	6/8	Age-related macular degeneration
4	52	F	6/5	6/6	Macular telangiectasia type 2
5	56	F	6/5	6/5	Proliferative diabetic retinopathy
6	38	M	6/5	6/12	Central serous chorioretinopathy
7	77	F	6/7.5	6/9	Macular telangiectasia type 2
8	30	F	6/6	6/6	Healthy control
9	33	M	6/6	6/6	Healthy control
10	27	M	6/6	6/6	Healthy control

F, Female; M, Male; BCVA, best-corrected visual acuity.

Table 2. Comparison of Retinal Vascular Tree Subbranches Visible between Conventional and High-Resolution FA

Participant	Conventional Image	High-Resolution Image	Difference
1	2	Poor quality	Not gradable
2	2	2	0
3	2	3	+1
4	3	4	+1
5	1	2	+2
6	2	4	+2
7	2	2	0
8	2	4	+2
9	2	4	+2
10	3	4	+1

the Topcon TRC-NW8, then the conventional HRA2 (Fig. 4). Similarly, high resolution ICGA demonstrated visualization of smaller caliber branches with greater appreciation of the spatial relationship between vessels (Figs. 5, 6). Across all participants imaged using the high-resolution device, however, there were variations in the clarity and fluorescence strength of the images obtained. In the first patient imaged, the high-resolution HRA2 image was of poor quality and ungradable, likely due to delayed timing of the imaging. Earlier onset of angiography imaging immediately after dye injection produced better quality images of the capillary network, compared to when imaging was delayed by >10 minutes.

In one patient who had high-resolution imaging performed in the foveal region, the diameter of retinal capillaries forming the FAZ boundary was calculated. The FAZ boundary was chosen for retinal capillary analysis to provide a benchmark location to compare against other studies. The mean diameter for capillaries at these four points was 8.2 ± 1.7 μm.

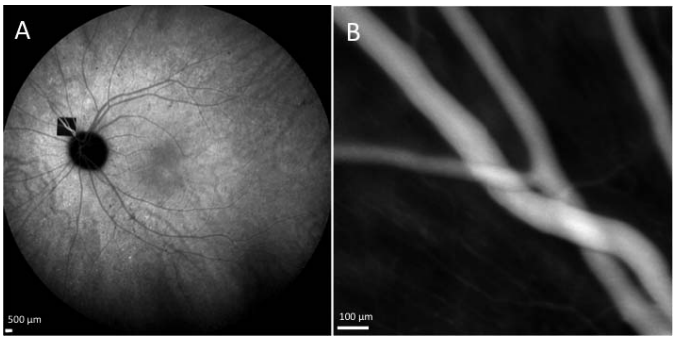

Figure 5. Localization (A) and (B) early phase high-resolution ICGA.

Aside from capturing static images, the HRA2 also can be used to take videos of the retinal vasculature in real time. No differences were seen on the videography setting when performing the high-resolution FFA or ICGA compared to the static images. However, when the modified device was set to continuous infrared mode, flow of blood cells was discernible, visualized as continuous movement within the retinal circulation (Supplementary Video).

Photoreceptor Mosaic Imaging and Analysis

High-resolution images of the photoreceptor mosaic also were acquired using the infrared and blue reflectance setting. Imaging of the cone photoreceptors was resolved to a level sufficient for automated and manual cone counting in both modalities (Fig. 7, cone density 7510 cells/mm^2 accounting for blood vessels, hexagonally packed cones 37.0%, mean cone spacing 13.9 ± 5.9 μm). Assessment of the photoreceptor density also could be obtained around microvascular structures of interest, such as a large microaneurysm in a diabetic patient (Fig. 8, cone

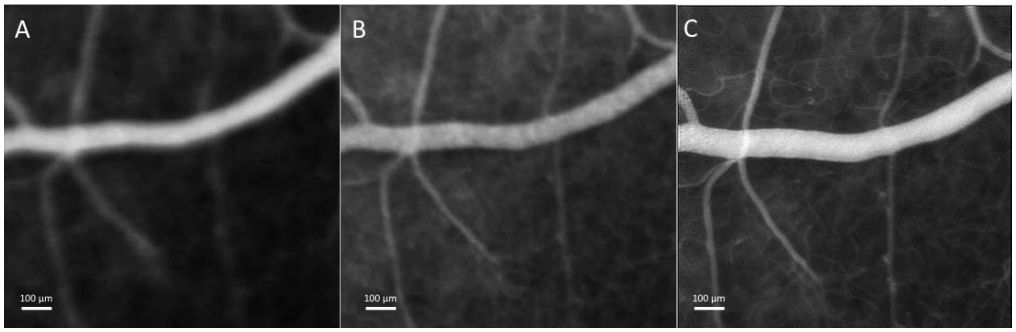

Figure 4. Comparison of enlarged conventional FFA on HRA2 (A), Topcon TRC-NW8 (B), and high-resolution HRA2 (C) in the same location.

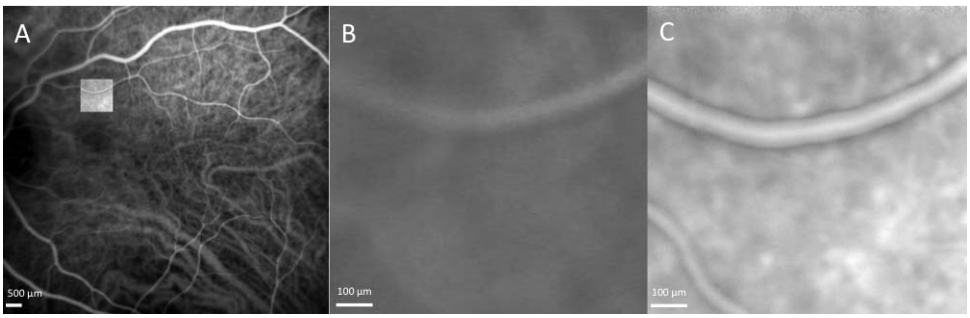

Figure 6. Localization and scaling of conventional ICGA image (A) with enlarged conventional (B) and high-resolution (C) images.

density in a region with microaneurysm of 11,645 cells/mm^2 compared to a region without microaneurysms 12,078 cells/mm^2). The device could be switched easily from infrared to angiography mode to provide an estimate of the cone density relative to perfusion in a given location (Fig. 9, cone density 8312 cells/mm^2 without blood vessels, hexagonally packed cones 45.5%, mean cone spacing 13.4 ± 7.5 µm).

Imaging of Choriocapillaris

In addition to standard angiography, the modified device also enabled imaging of the choriocapillaris layer by using the IRAF setting with ICG dye in situ. (Fig. 10).

Discussion

This study demonstrates that high-resolution in vivo fundus angiography is possible using nonadaptive optics imaging systems. Fine retinal capillaries and its subbranches were visualized with the narrow angle modification and there was improved spatial resolution of larger vessels on FFA and ICGA compared to conventional images. The system also was capable of demonstrating the topographic relationship between vessels and the photoreceptor mosaic on a single device, with cone density counts comparable to levels previously reported on AOSLO and histology.[13,14] In addition, the videographic capabilities of the modified HRA2 system were able to capture movement of blood cells through the retinal circulation in real time.

Our results are comparable to those obtained using AOSLO FA. In a study by Pinhas et al.,[7] FFA was performed using confocal AOSLO in 10 healthy subjects given oral or intravenous fluorescein dye. Compared to conventional FFA, confocal AOLSO FA demonstrated increased transverse and axial resolution and was able to resolve details of the retinal capillary bed. Although we did not perform AOSLO FA in our subjects, retinal images acquired using the modified HRA2 device in this study had potential resolution down to the same quaternary level branching and capillary network as seen in the confocal AOSLO FA report.[7] We also followed a similar method of analysis for the FAZ rim vessels to a previous report using AO OCT,[15] with our result of 8.2 µm in keeping with their published mean of 5.4

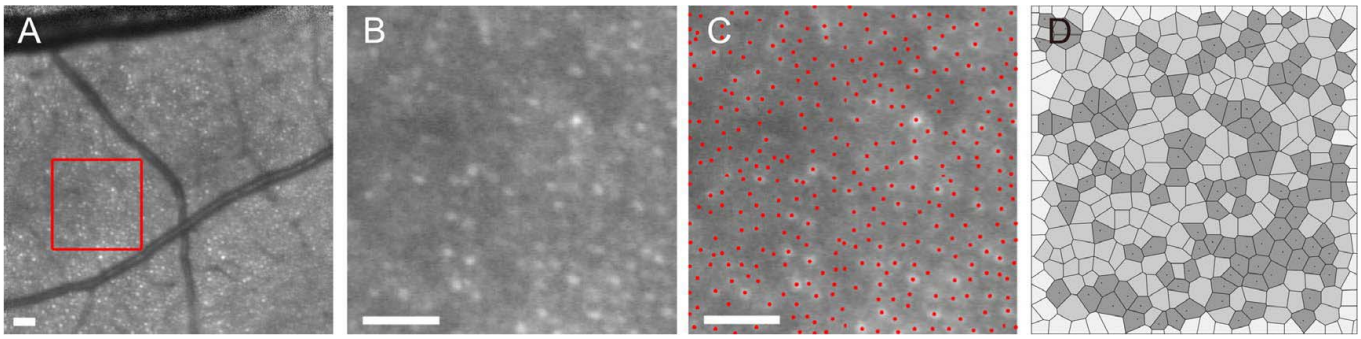

Figure 7. (A) High-resolution infrared image at 12° radial eccentricity focused at the level of photoreceptor mosaic. (B) Enlarged view of area of interest without blood vessels. (C) Cone density of 7510 cells/mm^2 (D) Voronoi analysis of cone packing arrangement. *Scale bar*: 50 µm.

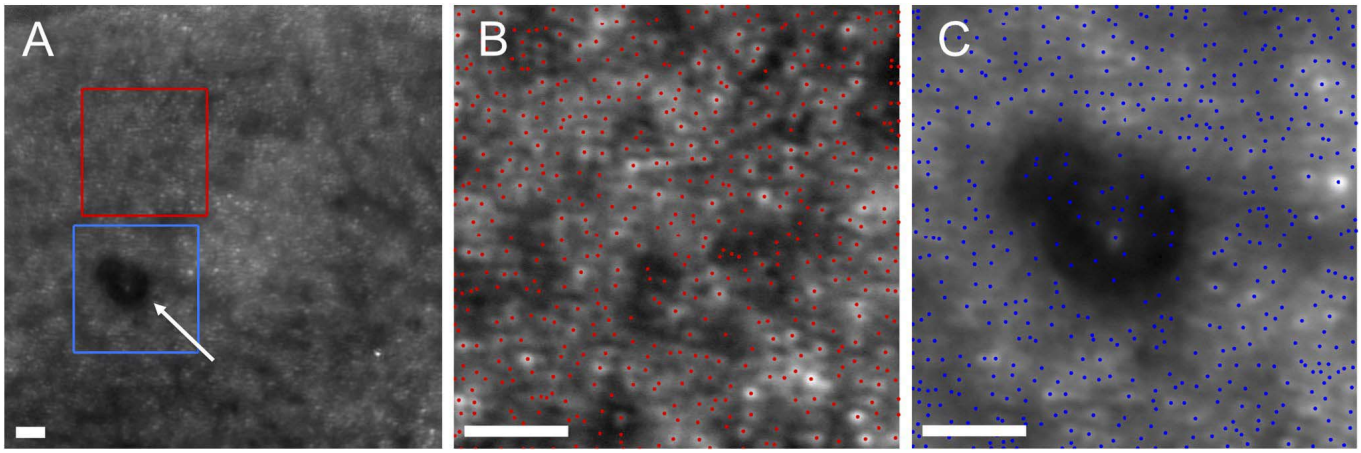

Figure 8. (A) High resolution infrared image at 8° eccentricity of a patient with diabetic retinopathy demonstrating large microaneurysm (*arrow*) measuring approximately 95 μm in its longest diameter and adjacent photoreceptor mosaic (*blue box*) and areas without microaneurysms (*red box*). (B) Cone density of 12,078 cells/mm^2 in area without microaneurysms and (C) 11,645 cells/mm^2 in area with microaneurysms. *Scale bar*: 50 μm.

μm. In addition, we also were able to measure the size of vascular features of interest, including a microaneurysm in one patient, with our en face diameter of 95 μm comparable to the mean 100 ± 57 μm longest intraluminal diameter for diabetic microaneurysms reported by Dubow et al.[8] using AOSLO FA.

The ability to resolve fine retinal capillary details using non-AO systems represents a significant advantage. Image acquisition using the high-resolution device is fast and can be viewed immediately without the need for complex image processing. In addition, the device is a modification of a conventional HRA2, a platform already familiar to many technicians, thus facilitating ease of use. It also can potentially be used to image a wider spectrum of patients including those with small pupils. However, AOSLO FA and the modified HRA2 require oral or intravenous dye administration to view the retinal vasculature.

Optical coherence tomography angiography is another imaging modality that can provide high resolution images of the retinal vasculature. It does not require dye injection and, as it is noninvasive, can be repeated at the same or multiple visits with good reproducibility.[16] Although limited in its field of view,

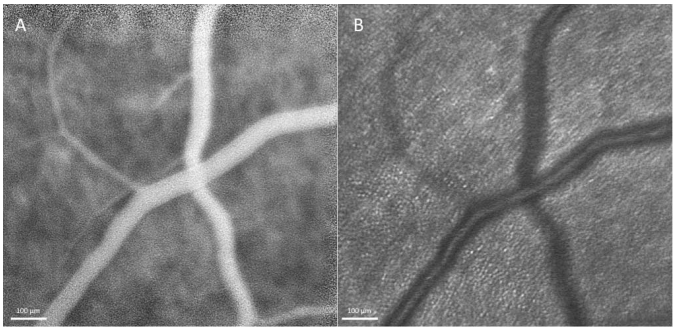

Figure 9. High-resolution FA images at 9° eccentricity (A) and infrared imaging of photoreceptor mosaic (B) at the same location (cone density 8312 cells/mm^2 in area without blood vessels).

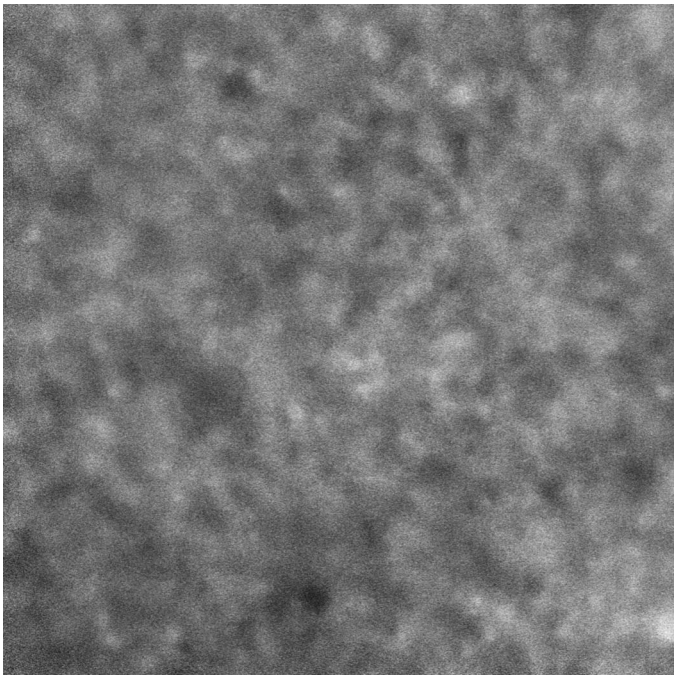

Figure 10. Imaging of choriocapillaris layer with high-resolution ICGA.

newer models in development are using montaging protocols to allow wider field images of up to 70°.[17,18] Compared to traditional dye-based angiography, such as this, however, its main disadvantage is its inability to demonstrate vascular leakage or areas of slow flow.

Limitations of this study include the small number of patients and the variation in the start time and fluorescence signal of the high-resolution FA due to the need to move patients from one device to another. To avoid subjecting patients to repeat angiograms, early phase images were captured only on one device at a time. A greater difference between the two devices may have been obtained if all the high-resolution imaging was performed in the early phase. There also were technical challenges in the reproducibility of the quality of the images. In addition, although the modified device provided improved visualization of smaller capillaries, the reduced field of view led to difficulties localizing where the image was being taken at the exact time of imaging. Montaging the images may help recreate a larger field of view; future modifications to the system to enable switching from the conventional to high-resolution scanning angle within the same device also would be desirable to allow rapid examination of targeted features. However, as an exploratory study, our results suggested the potential level of detail that can be obtained. Further studies, including early phase high-resolution FFA in all patients compared to either OCTA or FA AOSLO, and dedicated imaging of pathology, such as microaneurysms or neovascularization, will help clarify the scope of this technology.

The study of microvascular abnormalities remains vital to understanding the pathobiology of retinal vascular diseases. Advances in imaging technology such as this, which allow detailed in vivo assessment of the vascular network simultaneously with the surrounding neuroretina, have the potential to identify earlier manifestations of a disease and improve our understanding of the relationship between photoreceptors and retinal vasculature. This is important, not only for diagnostic purposes, but may have a role in phenotyping patients for novel future therapies. In addition, the ability to assess photoreceptor density alongside vascular abnormalities can provide insight into the relationship between the two, an important factor in determining the timing of intervention needed for disease prevention. This high-resolution FA technology provides a promising avenue to better understand microvascular changes in health and disease.

Acknowledgments

The authors thank Yoshihika Katayama and Heidelberg Engineering for their technical expertise with the HRA device.

Supported by the United Kingdom's National Institute for Health Research of Health's Biomedical Research Centre for Ophthalmology at Moorfields Eye Hospital and UCL Institute of Ophthalmology (AT, CE, RSA, and PJM). The views expressed are those of the authors, not necessarily those of the Department of Health. The funder had no role in study design, data collection, analysis, or interpretation, or the writing of the report.

Disclosure: **M. Okada**, Allergan (R), Bayer (R); **T.F.C. Heeren**, None; **P.J. Mulholland**, Heidelberg Engineering (C); **P.M. Maloca**, None; **M. Cilkova**, None; **V. Rocco**, None; **M. Fruttiger**, None; **C.A. Egan**, None; **R.S. Anderson**, Heidelberg Engineering (C); **A. Tufail**, Novartis (C), Roche (C), Allergan (C), Alcon (C), Heidelberg Engineering (C)

References

1. Novotny HR, Alvis DL. A method of photographing fluorescence in circulating blood in the human retina. *Circulation*. 1961;24:82–86.
2. Gao SS, Jia Y, Zhang M, et al. Optical coherence tomography angiography. *Invest Ophthalmol Vis Sci*. 2016;57:OCT27–OCT36.
3. Chui TYP, Mo S, Krawitz B, et al. Human retinal microvascular imaging using adaptive optics scanning light ophthalmoscopy. *Int J Retina Vitr*. 2016;2:11.
4. Roorda A, Romero-Borja F, Donnelly W, Iii Queener H, Hebert T, Campbell M. Adaptive optics scanning laser ophthalmoscopy. *Opt Express*. 2002;10:405–412.
5. Paques M, Meimon S, Rossant F, et al. Adaptive optics ophthalmoscopy: application to age-related macular degeneration and vascular diseases. *Prog Retin Eye Res*. 2018;66:1–16.
6. Chui TYP, Dubow M, Pinhas A, et al. Comparison of adaptive optics scanning light ophthalmoscopic fluorescein angiography and offset pinhole imaging. *Biomed Opt Express*. 2014;5:1173–1189.

7. Pinhas A, Dubow M, Shah N, et al. In vivo imaging of human retinal microvasculature using adaptive optics scanning light ophthalmoscope fluorescein angiography. *Biomed Opt Express*. 2013;4:1305–1317.
8. Dubow M, Pinhas A, Shah N, et al. Classification of human retinal microaneurysms using adaptive optics scanning light ophthalmoscope fluorescein angiography. *Invest Ophthalmol Vis Sci*. 2014;55: 1299–1309.
9. Matlach J, Mulholland PJ, Cilkova M, et al. Relationship between psychophysical measures of retinal ganglion cell density and in vivo measures of cone density in glaucoma. *Ophthalmology*. 2017;124:310–319.
10. Wolsley CJ, Saunders KJ, Silvestri G, Anderson RS. Comparing mfERGs with estimates of cone density from in vivo imaging of the photoreceptor mosaic using a modified Heidelberg retina tomograph. *Vision Res*. 2010;50:1462–1468.
11. Drasdo N, Fowler CW. Non-linear projection of the retinal image in a wide-angle schematic eye. *Br J Ophthalmol*. 1974;58:709–714.
12. Li KY, Roorda A. Automated identification of cone photoreceptors in adaptive optics retinal images. *J Opt Soc Am A Opt Image Sci Vis*. 2007; 24:1358–1363.
13. Park SP, Chung JK, Greenstein V, Tsang SH, Chang S. A study of factors affecting the human cone photoreceptor density measured by adaptive optics scanning laser ophthalmoscope. *Exp Eye Res*. 2013;108:1–9.
14. Jonas JB, Schneider U, Naumann GO. Count and density of human retinal photoreceptors. *Graefes Arch Clin Exp Ophthalmol*. 1992;230:505–510.
15. Wang Q, Kocaoglu OP, Cense B, et al. Imaging retinal capillaries using ultrahigh-resolution optical coherence tomography and adaptive optics. *Invest Ophthalmol Vis Sci*. 2011;52:6292–6299.
16. Spaide RF, Fujimoto JG, Waheed NK, Sadda SR, Staurenghi G. Optical coherence tomography angiography. *Prog Retin Eye Res*. 2018;64:1–55.
17. Hirano T, Kakihara S, Toriyama Y, Nittala MG, Murata T, Sadda S. Wide-field en face swept-source optical coherence tomography angiography using extended field imaging in diabetic retinopathy. *Br J Ophthalmol*. 2018;102:1199–1203.
18. Zhang Q, Rezaei KA, Saraf SS, Chu Z, Wang F, Wang RK. Ultra-wide optical coherence tomography angiography in diabetic retinopathy. *Quant Imaging Med Surg*. 2018;8:743–753.